Time Resolved Spectroscopy of Single Quantum Dots: Fermi Gas of Excitons?

U. Bockelmann,[1] Ph. Roussignol,[2] A. Filoramo,[2] W. Heller,[1] G. Abstreiter,[1] K. Brunner,[1,*]
G. Böhm,[1] and G. Weimann[1]
[1]*Walter Schottky Institut, Technische Universität München, Am Coulombwall, 85748 Garching, Germany*
[2]*Laboratoire de Physique de la Matière Condensée, Ecole Normale Supérieure, 24 rue Lhomond, 75005 Paris, France*
(Received 27 November 1995)

Photoluminescence measurements with spatial and temporal resolution are performed on individual GaAs/GaAlAs quantum dots. Already 10 ps after weak, resonant excitation, we observe luminescence which evolves to a spectrum of distinct, narrow lines. With increasing excitation intensity, the spectral weight shifts from the lowest to higher levels but the peak energies hardly change. Our results demonstrate that Coulomb scattering is an important relaxation mechanism and suggest that the interacting electron-hole plasma in quantum dots behaves like an exciton gas obeying Pauli exclusion. [S0031-9007(96)00141-X]

PACS numbers: 73.20.Dx, 78.47.+p

In quantum dots the charge carriers are confined in all three spatial directions and the energy spectrum is discrete, in analogy to the case of atoms. Energy levels of semiconductor quantum dots containing electrons have been studied by infrared absorption [1,2], resonant tunneling [3–5], and capacitance spectroscopy [2,6]. These experiments, which probe electrons in dots with nearly parabolic confinement, are insensitive to the many-body Coulomb interaction due to the so-called generalized Kohn theorem [7,8]. The determination of the energy spectrum from transport experiments is difficult because of charging effects.

In photoluminesence (PL) spectroscopy, electron-hole or exciton states are probed rather than the electron states. The experiment is sensitive to many-body effects, independently of the shape of the confinement potential. Sharp, discrete radiative transitions between quasi-zero-dimensional states in semiconductor structures are observed only in spatially resolved spectroscopy of individual quantum structures (see, for example, [9–12]). Without spatial resolution the measurements must be performed on arrays containing many structures which leads to a strong inhomogeneous broadening. In the experiment described in this paper, we have combined the spatial resolution with a time resolution of about 10 ps. This allows us to follow in the time domain the luminescence of the discrete states of single quantum dots. Up to now, time resolved PL experiments have been performed on arrays of quantum dots only. Individual lines are not resolved because of inhomogeneous broadening and a fast rise of the PL is observed, similar to results obtained with quantum wells [13,14].

There are important open questions regarding the energy relaxation in quantum dots. Theory predicts that in typical semiconductor quantum dots relaxation by phonon emission is efficient only between levels separated by no more than a few meV (via LA phonons) or by an energy within a few meV from a LO phonon branch (via LO phonons or a two phonon LO+LA mechanism) [15,16]. An experimental indication for this slowing down of relaxation in zero-dimensional (0D) structures is the appearance of narrow lines blueshifted with respect to the ground state in PL spectra collected on single GaAs/GaAlAs quantum dots under low power continuous wave (cw) excitation [9]. This contrasts to similar, more recent experiments on InAs dots, where the PL spectra have been interpreted in terms of a single line per dot [10]. In the presence of a sufficiently dense electron-hole plasma, typical for strong excitation conditions, relaxation by Coulomb scattering via an Auger mechanism is expected to become important in quantum dots [17]. This mechanism has not yet been demonstrated experimentally.

In addition to detailed information on the relaxation properties, our measurements also provide new insight into the energy spectrum of the interacting electron-hole plasma in quantum dots. We show that the spectrum and the temporal decay of the luminescence from this complicated few-particle system can be understood in terms of the single exciton properties of the quantum dot. Our approach includes the Pauli exclusion principle, a very unusual concept for excitons.

The measurements are performed on a series of quantum dot structures fabricated by laser-induced thermal interdiffusion of an undoped, 3 nm wide $GaAs/Ga_{0.65}Al_{0.35}As$ quantum well [9]. An individual dot structure is defined by drawing a square frame of size w with a focused Ar^+ laser on the sample surface. An area of 6×6 μm around the dot is interdiffused by scanning the beam continuously. Model calculations of the interdiffusion indicate that the lateral potentials are parabolic near the dot center with a barrier height of about 35 meV for both electrons and holes. The effective lateral confinement is given by the interdiffusion profile and not just by the geometrical size w. A splitting of the cw PL ranging from 0 to 10 meV is observed on a series of dot structures of different w. This splitting characterizes the strength of the lateral confinement. Details of the sample fabrication and the cw PL investigations are given in [9]. In this paper we discuss two structures: sample A with strong (10 meV splitting, $w = 450$ nm) and sample

 0031-9007/96/76(19)/3622(4)$10.00

B with weaker (4 meV splitting, $w = 500$ nm) lateral confinement. The other structures of the quantum dot series also exhibit much weaker line splittings than sample A and give qualitatively the same results as sample B.

The sample is locally excited with a wavelength-tunable, continuously mode-locked Ti:sapphire laser which generates 1.5 ps [full width at half maximum (FWHM)] pulses with a repetition rate of 82 MHz. The laser is focused through a microscope objective to a spot size of about 1.5 μm FWHM. All measurements presented in this paper are performed at a sample temperature of 7 K. The PL signal is dispersed through a 32 cm spectrometer and detected by a two-dimensional syncroscan streak camera with a spectral and temporal resolution of 2 meV and 10 ps.

Figure 1 shows time resolved PL spectra collected on the single quantum dot structure A. The luminescence is excited resonantly in the dot, below or above the threshold energy for LO phonon emission into the ground state ($\hbar\omega_{\mathrm{LO}} = 36$ meV in GaAs). The PL signal appears with a rise time τ_r of about 10 ps, close to the time resolution of the experiment. This holds for the whole spectrum, at all excitation intensities (140 nW–14 μW) and all excitation energies (18–66 meV above the ground state). Within the first 50–100 ps the spectra are broadened to an amount which increases with the pulse power. The short rise time, the independence on the excitation energy (above or below the LO phonon energy), and the density dependent broadening show that Coulomb scattering is important in the early stage of thermalization. Scattering by LA phonons is too slow to explain the small value of τ_r [18]. For relaxation dominated by LO phonon emission alone, we would expect strong effects when the excitation energy is scanned through $\hbar\omega_{\mathrm{LO}}$. Neither the rise time nor the spectra show a systematic dependence of this kind. Apparently, Coulomb scattering, which can promote a part of the charge carriers above $\hbar\omega_{\mathrm{LO}}$ and with that allows for LO phonon emission even for an excitation below $\hbar\omega_{\mathrm{LO}}$, is efficient down to the smallest laser power of 140 nW. These conclusions hold for all investigated dot structures.

For sample A, at long time delays, the spectra consist of a set of distinct peaks. The number and relative weight of these lines depend on the laser power, as shown in Fig. 2. For an excitation power of 450 nW, two main peaks separated by about 10 meV are observed; the spectrum is very similar to the ones measured with weak cw excitation [9]. With increasing power of the resonant pulsed excitation, two strong, additional lines appear at higher energy and the spectral weight shifts systematically to these excited states. For sample B, the individual lines are hardly resolved in the time resolved measurement because the lateral confinement is much weaker. Accordingly, the blueshift of the spectral weight with increasing power is smaller than in sample A.

The exciton number in the dot N_{ex}, excited by one pulse, is estimated as $N_{\mathrm{ex}} \cong \alpha\gamma N_{\mathrm{phot}}$. The number N_{phot} of photons which impinge on the sample follows directly from the measured average laser power P via $N_{\mathrm{phot}} = P/\nu\hbar\omega$ (photon energy $\hbar\omega$, repetition rate $\nu =$ 82 MHz). The factor γ describes the portion of the laser spot profile on the actual dot size. An absorption probability of $\alpha = 6 \times 10^{-3}$ is used, as a typical value for GaAs quantum wells. For the 1.5 μm spot on the structure with a geometrical size of $w = 450$ nm, we thus obtain 12.5 excitons per pulse in the dot for 1 μW laser power. For the power range of Fig. 2, the estimate gives from 170 down to about 2 excitons per pulse on average.

Let us now consider the dependence of the peak positions on the excitation power, i.e., the estimated exciton number N_{ex}. The lowest two lines, which dominate at weak excitation, shift by about 1 meV to smaller energy when N_{ex} increases from 1.7 to 56. The position of the two higher levels is independent of N_{ex}, within the spectral resolution. The remarkably weak energy shifts strongly suggest that the photoexcited carriers are well described as an exciton gas over the whole range of N_{ex}. The state filling effect indicates Fermi statistics. A Fermi gas of excitons? Let us first quantify this approach before we show that it can also explain the temporal decay of the PL spectra.

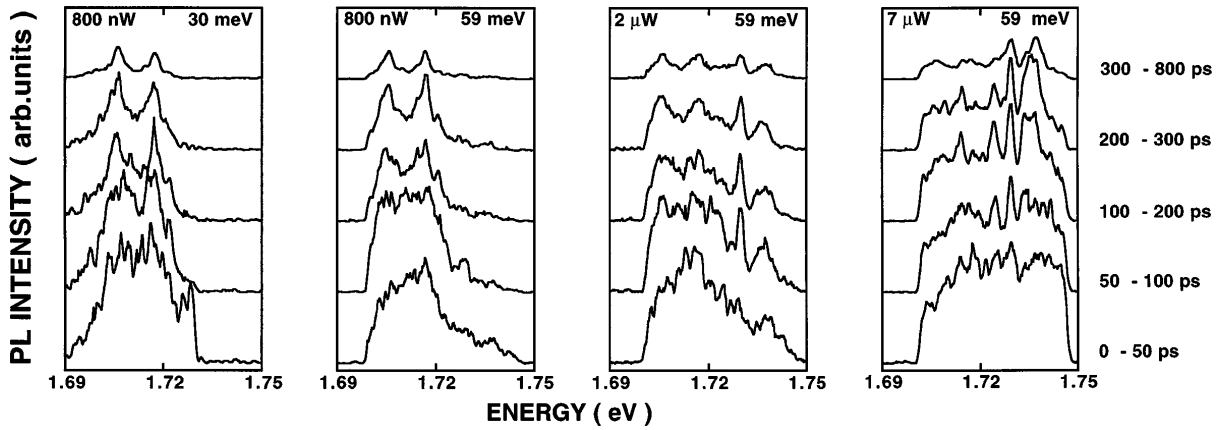

FIG. 1. PL spectra of sample A for different time delay windows. The excitation power, focused to a 1.5μm spot, is given at the top left. Excitation is within the dot, 59 or 30 meV above the lowest PL peak, as indicated on the top right.

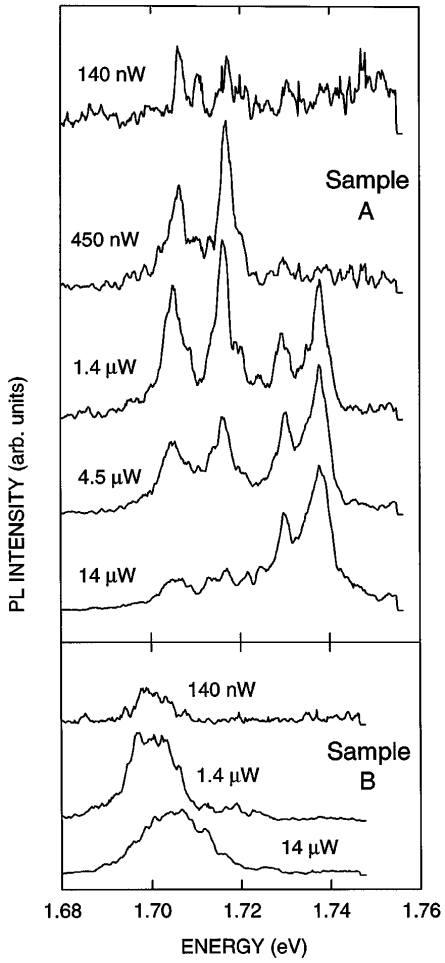

FIG. 2. PL spectra integrated over times of more than 250 ps after the pulse. Excitation is provided at 1.764 eV. The spectra are normalized to the excitation power.

A theoretical description of single exciton states in the dots under study has been developed in [18]. The right part of Fig. 3 shows the calculated level scheme of heavy hole excitons in a model potential for samples A and B. Excitonic effects are very important in our dot structures because the exciton binding and lateral confinement energies are comparable. The dominant radiative levels are almost equidistant and their recombination rates are similar. The Fermi energy E_F of an exciton gas, defined by filling in turn the discrete levels, is given by the left curves. The confinement potential in a real structure will certainly differ from the parabolic and rotational symmetric model potential. Such a deviation can be due to charged defects introduced by the laser processing in the surrounding area or simply by not perfectly constant interdiffusion conditions during writing the square frame which defines the dot. It mixes energetically neighboring states and nonradiative excitons gain oscillator strength. We therefore expect more radiative states in the real structures, but the oscillator strength should remain centered around the dominant radiative states of Fig. 3. In any case, the real energy spectrum is discrete and the dependence of E_F on N_{ex} is, as a property of the level statistics, not very sensitive to a perturbation of the confinement potential.

The shift of E_F by more than 30 meV with N_{ex} increasing from 1 to 100 shows that the appearance of the two higher energy peaks in sample A is consistent with the occupation of the discrete states from below. The lowest states first acquire a sizable occupation and the level degeneracy is higher at the excited state transitions. As a consequence, the lower peaks saturate at intermediate power levels, while the upper ones increase linearly with P up to 14 μW. For weaker lateral confinement (ω_e = 2 meV) the increase in E_F is smaller, in accordance with the smaller blueshift observed on sample B.

For the investigated quantum dots, theory predicts that LA phonon scattering between exciton states separated by more than about 5 meV becomes inefficient on the time scale of radiative recombination (Fig. 2 of [18]). In sample A relaxation from the first excited radiative state is hindered, but excitons at higher energy can relax using the closely spaced nonradiative levels (Fig. 3). This explains

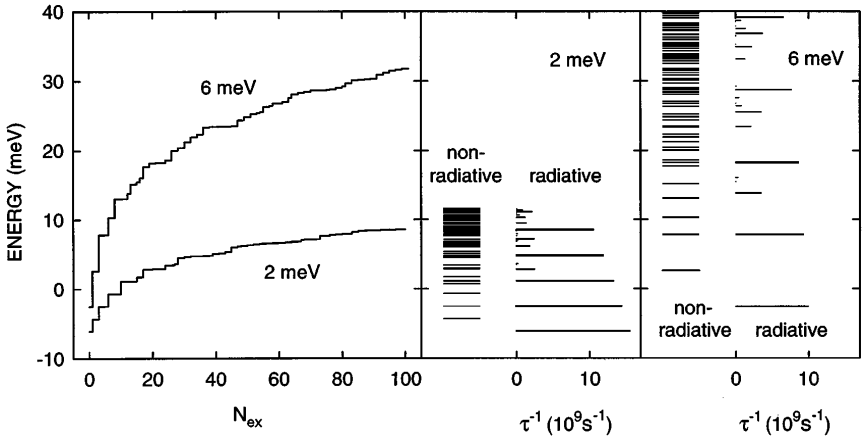

FIG. 3. Calculated energies and radiative lifetimes of excitons in quantum dots. The parabolic lateral potential is characterized by the separation $\hbar\omega_e$ of the single electron states. The value $\hbar\omega_e$ = 6 meV (2 meV) corresponds to sample A (B). The inverse recombination time τ^{-1} of the radiative states is given by the length of the horizontal bars, through the bottom scale. The left part shows the Fermi energy E_F as a function of the number of excitons N_{ex} in the dot, at zero temperature.

why for low excitation power the ground and first excited transitions are observed but not yet the two higher energy lines. The latter appear only at stronger excitation where the relaxation from the higher radiative states decreases by an increasing occupation of the states below. To achieve a sizable occupation, the thermal energy kT of the exciton gas should not exceed its Fermi energy E_F. Therefore it is favorable, first, to have a small density of states (ideally a quantum dot of large level spacing) in order to obtain a sizable E_F already at low excitation power and, second, to excite resonantly in order to avoid heating by a high excess energy. As a consequence, sample A, which exhibits the smallest density of states, is predestined to form a degenerate Fermi gas.

In Fig. 4, we compare the time evolution of the PL spectra of samples A and B, under the same excitation conditions. In sample A the excited state transitions exhibit comparable or even longer decay times than the ground state, showing the absence of efficient relaxation expected for the degenerate Fermi gas. This contrasts sample B. There is a clear transfer of intensity with time from higher to lower energy, the decay time decreases with increasing energy. In sample B, the density of states is too high to achieve a degenerate Fermi gas and therefore the Pauli blocking of the relaxation is less efficient. That the energy distribution is more classical in this case also appears directly from the spectra in the insets.

In addition, we have theoretically studied the energy relaxation of the exciton gas in the quantum dots. A rate equation, based on calculated exciton LA phonon scattering and radiative recombination times, is solved. A Fermi initial distribution characterized by the exciton number N_{ex} and temperature T_{ex} is assumed as a simple model for the system shortly after the initial stage of fast relaxation. For the example of $N_{ex} = 50$, $T_{ex} = 4$ meV and considering the Pauli exclusion principle, we obtain independent recombination of the lines for strong (sample A, $\hbar\omega_e = 6$ meV) and an internal dynamics for weak (sample B, $\hbar\omega_e = 2$ meV) lateral confinement, in agreement with the experiment. On the other hand, without Pauli exclusion a pronounced internal dynamics is calculated both for weak and strong confinement.

In summary, time resolved microscopic PL spectroscopy has been performed on individual quantum dot structures. We find that Coulomb scattering is important in the carrier relaxation process, down to very low excitation power. The interpretation in terms of a Fermi gas of excitons describes the whole set of experimental results: the systematic change of the spectra with increasing laser power, the Pauli blocking of the relaxation, and the qualitative differences between strong and weak lateral confinement. The concept of a Fermi gas of quantum dot excitons is an interesting subject for futures studies. Experimental investigations on quantum dots fabricated by other techniques could provide information about the generality of the results with respect to the shape of the confinement potential. On the theoretical side, we need a microscopic understanding why the observed behavior of the correlated electron-hole plasma in the quantum dots can be interpreted in terms of single exciton properties.

We are pleased to thank C. Delalande, J. Y. Marzin, B. Ohnesorge, P. Voisin, and M. Voos for their support, helpful suggestions, and discussions. One of us (A. F.) thanks the European Community for financial support (Human Capital and Mobility Grant No. ERBCHBICT 930654). The work has been supported financially by the Deutsche Forschungsgemeinschaft (Grant No. SFB348) and by a PROCOPE contract.

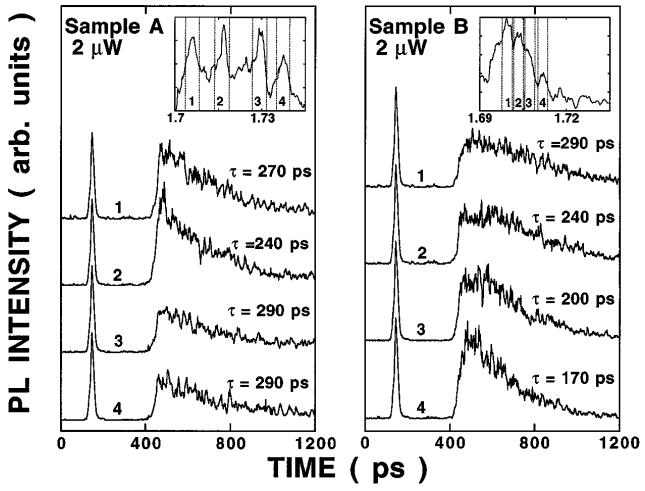

FIG. 4. Time dependence of the PL intensity from different spectral windows. The spectrum in the inset is integrated over times of more than 500 ps after the excitation pulse for sample A (600 ps for B). Excitation is provided at 1.767 eV. The values of τ are obtained by fitting the temporal decay of the PL. The sharp peaks at 150 ps show the laser pulse from a delay line.

*Present address: MPI für Festkörperforschung, Stuttgart, Germany.

[1] Ch. Sikorski *et al.*, Phys. Rev. Lett. **62**, 2164 (1989).
[2] H. Drexler *et al.*, Phys. Rev. Lett. **73**, 2252 (1994).
[3] M. A. Reed *et al.*, Phys. Rev. Lett. **60**, 535 (1988).
[4] P. L. McEuen *et al.*, Phys. Rev. Lett. **66**, 1926 (1991).
[5] A. T. Johnson *et al.*, Phys. Rev. Lett. **69**, 1592 (1992).
[6] R. C. Ashoori *et al.*, Phys. Rev. Lett. **71**, 613 (1993).
[7] L. Brey *et al.*, Phys. Rev. B **40**, 10 647 (1989).
[8] K. Karraï *et al.*, Phys. Rev. B **40**, 12 020 (1989).
[9] K. Brunner *et al.*, Phys. Rev. Lett. **69**, 3216 (1992).
[10] J.-Y. Marzin *et al.*, Phys. Rev. Lett. **73**, 716 (1994).
[11] H. F. Hess *et al.*, Science **264**, 1740 (1994).
[12] K. Brunner *et al.*, Phys. Rev. Lett. **73**, 1138 (1994).
[13] G. Wang *et al.*, Appl. Phys. Lett. **64**, 2815 (1994).
[14] J. M. Gérard, in *Confined Electrons and Photons: New Physics and Applications*, edited by C. Weisbuch and E. Burstein, NATO ASI, Ser. B, Vol. 304 (Plenum Press, New York, 1995), p. 357.
[15] U. Bockelmann *et al.*, Phys. Rev. B **42**, 8947 (1990).
[16] T. Inoshita *et al.*, Phys. Rev. B **46**, 7260 (1992).
[17] U. Bockelmann *et al.*, Phys. Rev. B **46**, 15 574 (1992).
[18] U. Bockelmann, Phys. Rev. B **48**, 17 637 (1993).